図3　図2症例の水平断の脳

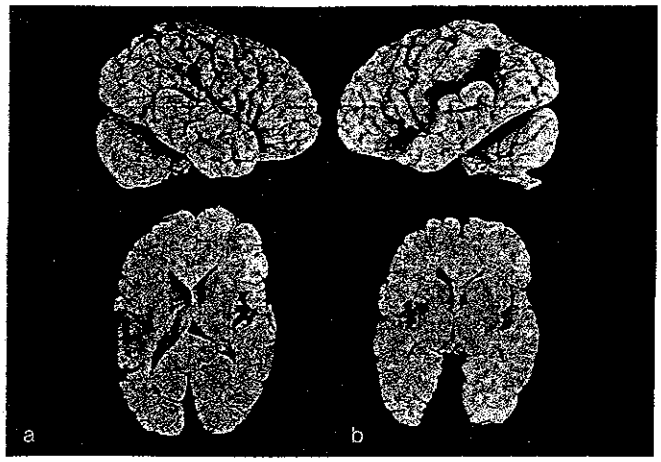

a．左半球の聴皮質はほとんど消失しているが，右半球の聴皮質はシルヴィウス裂側に部分的な損傷を認める．
b．左半球の側頭葉の損傷が大きい．

図4　図2症例の左右の内側膝状体組織学的像

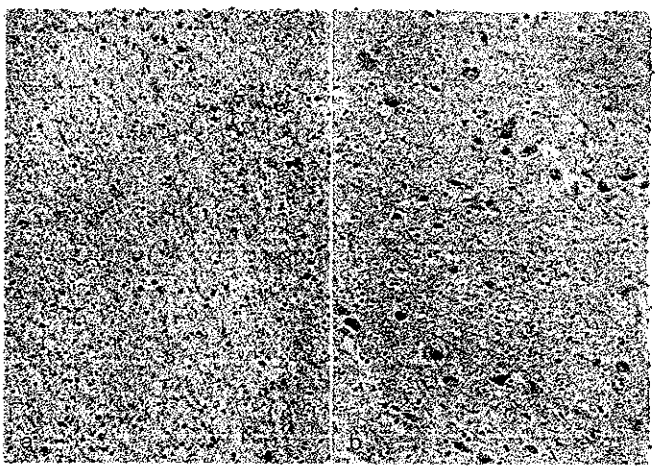

HE染色，＃9
a．左半球の内側膝状体．完全にニューロンが消失し，グリアに置き変わっている．
b．右半球の内側膝状体．ニューロンが割合保存されている．

ーロンがその線維である聴放線の障害により，変性をきたすためである(図3，4)．

筆者らの聴覚失認の症例の剖検脳とその病理組織像は，左の聴皮質は完全に欠損しているが，その同じ半球側の内側膝状体のニューロンは完全に脱落している．しかし，右の聴皮質は部分的に破壊されているだけで内側膝状体のニューロンの多くは保たれている．これまでの聴覚失認の剖検例の内側膝状体の病理所見では，ほとんどの症例でニューロンがグリアに置き換わっている．

【語音聴力検査と語音認知】

単音節の認知そのものである語音聴力検査は全くできない．最高明瞭度は10％以下でチャンスレベルである．単語や短文の認知も同様にできない[4]．

【聴覚的理解】

トークンテストおよび標準失語症テストの聴覚項目の検査を用いるが，ほとんどができない．しかし，このような状態であっても読話を併用すると，少しではあるが向上することがある．ただし，実際の生活の場では1対1の話し合いのときに，まれに読話を利用する程度である[4]．

【環境音テスト】

環境音の認知は手がかりがなければほとんどできない．現在のところ標準化された環境音テストはないが，筆者と杉下は，非言語音の認知の中枢処理過程のメカニズムを知るためには，テスト音について検討が必要であると考え，20項目の環境音テストを作成した．vocalizationという概念を導入し，言語音以外のnonvocalizationに分けて用いている．聴覚失認では，裸耳のみの聞き取りテストはほとんどできない．しかし，4つの絵カードのなかから選ぶ課題であれば可能なものがある．たとえば太鼓である．いわば言葉のdistinctive featureのような属性が環境音にもあり，それが手がかりとなって正答を得るのであろう[4]．

【音楽認知のテスト】

音の3要素であるピッチ，強度，長さ，および音楽の3要素であるメロディ，リズム，ハーモニーと音色の認知は著しく障害される．音楽の場合は時間因子が大切な要素であるが，time resolutionの認知障害のためメロディの認知はできない．しかし簡単なリズムは認知できる．不思議なことに音楽の情緒面，すなわち悲しい，楽しい，行進曲風などはわかることがある．ある症例では，この音楽の要素のテストは全く正解が得られなかったのにもかかわらず，音楽の情緒のテストは正解であった．音楽の情緒面は聴皮質を介さなくとも，非特殊聴覚伝導路や恐らく大脳辺縁系を介して可能であることを示唆する．

【Familiar Voice Testと Emotional Voice Test】

Familiar Voice Testとは慣れ親しんだ声のテストで，言葉の情緒のテストと，親しいヒトの声を当てさせる弁別テストがある．言葉の情緒のテストは「太郎！」と呼ぶときに，"怒り"，"親しさ"，

263-00096

"悲しみ"などの抑揚をつけ，これを区別させるものである．ほかに，患者の世代の経験した総理大臣・歌手・俳優などの声を区別するテストや家族の声の認知テストである．言葉の認知理解の全く困難な聴覚失認症例の家族の声のテスト結果は，全部正解である例があった．個人の声のもつイントネーションや声の色のような属性も，聴皮質を介さなくとも認知可能と考えられる．このようなテストは，わが国ではまだ実施されていない[4]．

【方向感覚テスト(Sound Lateralization Test)】

聴覚失認例の日常生活では，音源定位ができるか否かが問題である．交通事故が心配であるが，そのような事故の報告はまだない．ただし，方向感覚テストでは両耳時間差の認知は全くできないが，両耳強度差の閾値は上昇しているが認知できることがある．このことは，日常生活における方向感覚は時間差は失われても強度差はかなり認知できることを示唆している[4]．

最近の研究の進歩

(1) 画像診断[4]

CT・MRIの臨床応用がなされるようになって，内側膝状体・聴放線・聴皮質の損傷が容易に正確に同定できるようになった．ヘルペス脳炎の小児のCTでは両側側頭葉の壊死像を認める[5]．

聴皮質およびウェルニッケ中枢は，中大脳動脈の灌流枝の支配である．その流域枝の梗塞あるいは破綻で，聴皮質あるいは聴放線の損傷が生じる．なお，内側膝状体の灌流枝は後大脳動脈である．脳血管障害による聴覚失認では，CTでは脳梗塞像，3DCTアンギオでは左右の中大脳動脈の側頭葉への灌流枝の閉塞像を認める．聴覚失認例(両側聴放線障害)のポジトロンCT(PET)では，音刺激で残存聴皮質の血流が増加するか否かが評価できる．PETでは聴放線損傷でも聴皮質に血流が増加するので，非特殊聴覚系から聴皮質に投射する神経路があると思われる．しかし，その役割は大きくはない．

(2) 聴性誘発電位

聴性脳幹反応(ABR)は正常反応を示し，聴性中間反応(MLR)は正常，あるいは異常の両方があり，頭頂部緩反応(SVR)は正常反応を示す．2音を弁別課題とする事象関連電位のP300は出現しないが，視覚との組み合わせのCNV(contingent negative variation)は出現する．実際にはABRを末梢・脳幹の障害の有無のチェックに使い，MLRとSVR聴皮質の指標に使う[6]．

図5　脳磁図(MEG：a)と誘発電位(EEG：b)の同時記録

正常例．中間潜時反応は聴皮質に電流源を認める(○印)

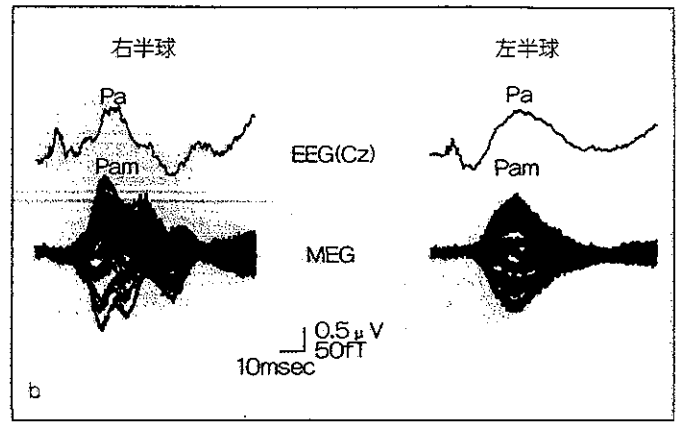

(3) 脳磁図(MEG)

脳磁図(magnetoencephalogram；MEG)は神経細胞の主に興奮性後シナプス電位によって生じる磁界を頭皮により記録したものである．磁界の発生源として最も重要な神経細胞は，大脳皮質の錐体細胞である．MEGにおいてもEEGによる誘発電位と同様に，誘発磁場が記録できる[6]．MEGのほうが局在性がはっきりしている．

【中間潜時反応】

MLRに相当する反応に中間潜時聴性誘発磁気反応(middle-latency auditory evoked magnetic field；MLAEMF)がある．誘発電位のMLRをE-MLRとあらわしMLAEMFと比較するとNaがN9m，PaがP30m，P1すなわちPbがP60mとなる．筆者らの研究ではMLAEMFの陽性ピークをPamとすると潜時は左耳刺激右半球記録では

図6　脳磁図と誘発電位

左の側頭葉損傷(＊印)．損傷側では中間潜時反応は消失，健側は出現．

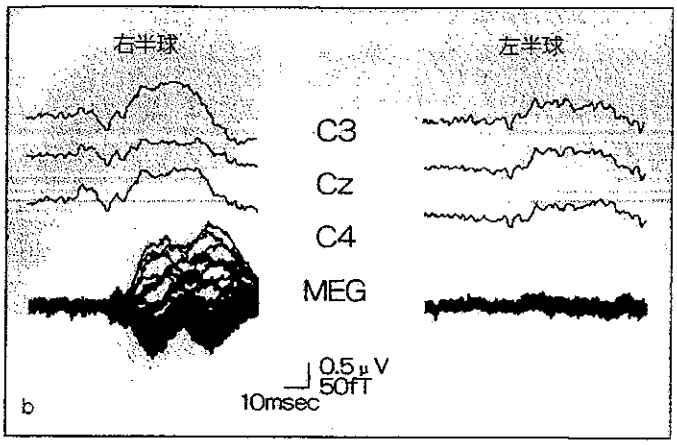

図7　脳磁図と誘発電位

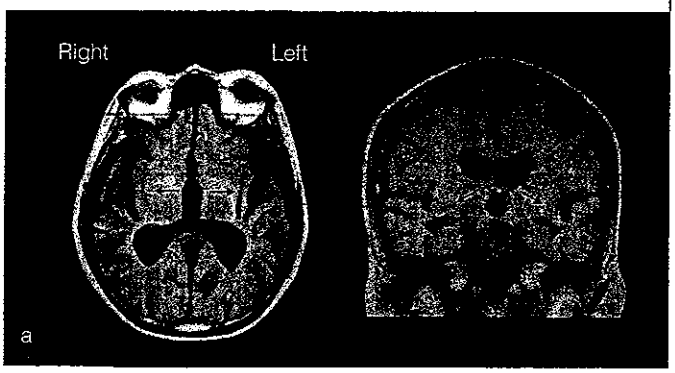

両側の聴放線損傷(矢印)による聴覚失認．中間潜時反応は両側の半球とも．PaもPamも消失．

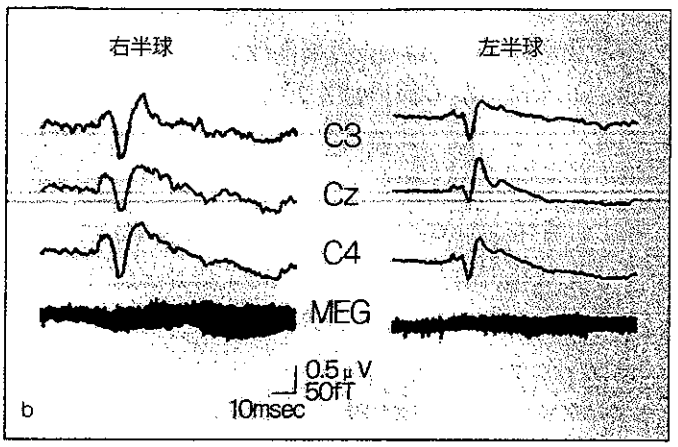

34 ± 7.0 msec，右耳刺激左半球記録では32 ± 7.0 msecで，E-MLRのPaと1～2 msecの差しかない．正常側ではPamの電流源は左右半球とも双極子が聴皮質上に位置する(図5)．聴皮質に損傷のある側では反応が消失する(図6)[7]．これは左右半球のいずれも同様である．以上のように聴皮質損傷の機能的評価はE-MLRよりMLAEMFのほうが原理的にも臨床的にも合致している．

以上のようにE-MLRとMLAEMFは波形は似ているが異なるものであり，聴皮質の損傷の機能診断には中間潜時反応は脳磁図を利用するほうが部位の同定が正確であり好ましい．

【緩反応(Slow Vertex Response；SVR)】

欧米ではLong Latency Responseと呼ばれ，わが国ではSlow Vertex Responseと慣習的に呼ばれている．脳波のK complexを加算したもので，N1，P1，N2，P2からなる．睡眠の深さによって振幅が変化するため実用的とはいえず，ABRにとって代わられた．ところが1990年代になり聴覚誘発脳磁界が記録されるようになり一変した．音刺激後，約100 msecにN1m(脳磁図によるN1はmをつけて電気的反応のN1と区別する)が側頭葉近傍上に聴覚誘発脳磁界が測定され，反応磁界が頭部から出てくることを示す．このN1mの脳磁界のMRI上に等価電流双極子を投影すると聴皮質上に位置する．電流の向きは聴皮質面に垂直で下方を向いており，その強さは数nAmから数十nAmである．Makelaらは聴覚野およびその近傍に損傷をもつ側では損傷が上側頭面の内側に及ぶとN1mが消失するがHeschl回転に損傷があっても聴放線が正常であれば正常なN1mが記録されたという．しかし，聴放線が両側とも損傷されると出現しない(図7)．このように，中枢性聴覚障害の他覚的機能診断にはMEGは新しい有効な武器であることがわかる．

電気的反応のN1と脳磁図のN1mは見かけ上も潜時も類似しているが，その起源は異なる．MLAEMFのPamとN1mは共に聴皮質に起源をもつが前者はより内側に，後者はより外側に双極子をもつと考えられている．

263-00096

今後の展望

聴覚失認では，両側の聴皮質あるいは聴放線が損傷されているにもかかわらず，聴覚作用は完全に失われることはない．その残存聴覚と読話の併用によってコミュニケーションが改善されることもあるがそれはわずかの効果しかなく実用的ではない．残存聴覚作用は脳のどの部位で認知されているのか，単なる反射作用なのか，まだわかっていない．筆者はHeschl回転以外にも大脳に副次的な聴皮質の存在がありうると推測している．このようにもう一つの聴覚神経系は脳のどこにあるかを明らかにすることが大きな課題として投げかけられている．

文　献

1) Wernicke C, Friedlander C：Ein fall von Taubheit in Folge von doppelseitiger laesion des Schlafellappens. *Fortschritte der medizin* 1：177-85, 1883.
2) 加我君孝：聴覚皮質中枢とその障害．東京医学 **100**：10-20，1993.
3) 加我君孝：両側聴皮質・聴放線損傷と純音聴力閾値．*JOHNS* **15**：23-33，1999.
4) 加我君孝(編)：中枢性聴覚障害の基礎と臨床，金原出版，2000.
5) 加我君孝：聴覚誘発電位の起源．神経進歩 **46**：110-127，2002.
6) Kaga K, Kaga M et al：Auditory agnosia of children after herpes encephalitis. *Acta Otolaryng* **123**：232-235, 2003.
7) Kaga K, Kurauchi T et al：Auditory middle latency MEG of patients with unilateral auditory cortex lesion. *Acta Otolaryng*. in press.

Acta Otolaryngol 2004; 124: 376–380

Taylor&Francis
healthsciences

Middle-latency Auditory-evoked Magnetic Fields in Patients with Auditory Cortex Lesions

KIMITAKA KAGA, TAKAHIDE KURAUCHI, MASATO YUMOTO and AKIRA UNO

From the Department of Otolaryngology, Graduate School of Medicine, University of Tokyo, Tokyo, Japan

Kaga K, Kurauchi T, Yumoto M, Uno A. *Middle-latency auditory-evoked magnetic fields in patients with auditory cortex lesions.* Acta Otolaryngol 2004; 124: 376–380.

Objective—To demonstrate the influence of auditory cortex lesions on auditory middle-latency responses (AMLRs) and middle-latency auditory-evoked magnetic fields (MLAEFs) in humans.

Material and Methods—A total of 15 normal subjects, 9 patients with left auditory cortex lesions and 1 patient with a right auditory cortex lesion were studied. MLAEFs were recorded from each hemisphere of the brain in a magnetically shielded room using a 37-channel SQUID gradiometer. Simultaneously, AMLRs were recorded from the scalp at the vertex, C3 and C4. Tone bursts were used as auditory stimuli.

Results—Pam responses of the MLAEF, which are typically evoked in the latency range of the Pa of the AMLR, and are localized at the auditory cortex as dipoles, were impaired or abolished over the left auditory cortex lesion in the patients with left-hemisphere lesions, but the Pa of the AMLR persisted.

Conclusion—The main generator of the Pam in MLAEF was demonstrated to be the auditory cortex. The results also show that the Pa of the AMLR is evoked only partly from the auditory cortex. *Key words: auditory cortex lesion, auditory middle-latency response, magnetencephalography, middle-latency auditory-evoked magnetic fields.*

INTRODUCTION

The generators of auditory middle-latency responses (AMLRs) have been a subject of controversy in animal experiments (1, 2) and clinical studies (3–5). The critical issue is whether or not the auditory cortex contributes to the AMLR. The AMLR has been used for functional diagnoses in patients with auditory imperception, such as word deafness or auditory agnosia (4). However, an important issue with AMLR recording is that Pa, a major AMLR component which is observed with a latency of 50 ms, did not disappear in all reported patients with auditory agnosia due to bilateral auditory cortex lesions (4).

The conventional MLR, which is recorded from the patient's scalp, is a far-field recording of electric potential differences generated by neural currents. The signal is significantly affected by the intervening tissues, such as the scalp, cranial bones and cerebrospinal fluid. Also, multiple generators cannot be isolated in such recordings. In contrast, in magnetencephalography (MEG) the magnetic field generated by the electric current in neurons is measured. As the magnetic permeability of the intervening tissue is almost the same as that of air, the magnetic field can be measured on the surface of the scalp with little distortion. MEG is particularly effective in localizing signals from axons that are oriented perpendicular to the scalp, such as those in the cortex and its projections. Its precision in mapping such generators is enhanced by the fact that the field strength from these sources falls rapidly with distance (6, 7). Therefore, MEG is suited to the precise localization of the activity sources in the brain. As an indicator of auditory cortex function in MEG, the N1m is widely used for basic and clinical studies (8, 9). There have been only a few studies of the Pam of middle-latency auditory-evoked magnetic fields (MLAEFs), which are also localized in the auditory cortex (10–13), and no auditory cortex lesion study of the Pam of MLAEFs has been reported.

The aim of this study is to demonstrate the influence of auditory cortex lesions on the Pa of AMLRs and the Pam of MLAEFs using simultaneous recordings in patients with such lesions.

MATERIAL AND METHODS

Subjects

Normal subjects comprised 10 males and 5 females (mean age 31.5 years). Also studied were nine patients with left auditory cortex lesions and one with a right auditory cortex lesion. All auditory cortex lesions were caused by cerebrovascular accidents and involved unilateral temporoparietal damage.

Methods

MLAEFs were recorded in a magnetically shielded room using a 37-channel SQUID gradiometer (Magnes; Biomagnetics Technologies). The patient was recumbent on a bed with his/her head fixed by a vacuum cushion. Auditory stimulation was provided by tone bursts (2000 Hz; 100.2 dB peSPL; rise/fall time 0.1 ms; plateau 10 ms), which were delivered to 1 ear of the subject through a plastic tube. The stimulus rate was 2 Hz, with 3000 repetitions. The sensor array (144 mm in diameter) was located as close as possible to the auditory cortex on the side opposite to the stimulated

 ISSN 0001-6489

DOI 10.1080/00016480310000647

ear. MLAEFs from the right and left cerebral hemispheres were recorded separately. Simultaneously, AMLRs were recorded using surface electrodes placed at Cz (vertex), C3 (over the left temporal lobe) and C4 (over the right temporal lobe). The ground electrode was placed on the ear lobe of the stimulated ear. The recording bandwidth was 1–2000 Hz. The peak latency (milliseconds) and amplitude [root-mean-square (r.m.s.) value in the case of the MLAEF] were measured.

Equivalent current dipoles (ECDs) were estimated at 0.96-ms intervals based on the magnetic field data obtained at each measurement point. ECDs are a collection of hypothetical dipoles that would produce the pattern of the magnetic field recorded at a particular point in time. Each ECD is represented as a vector, i.e. having an origin and direction within the brain, and a strength. A correlation coefficient is calculated between the predicted field for each ECD and the actual magnetic field pattern. Among the ECDs at each latency, that with the highest correlation coefficient was selected as a Pam current source (hereafter ECD refers to the ECD with the highest correlation coefficient). ECDs were judged reliable when their correlation coefficients were > 0.98, and brain MRI overlays were performed only for the reliable ECDs. The position of an ECD was represented in a coordinate system.

Brain MRI scans were obtained using an image scanner (Sharp JX-600) and transferred to a data analysis processor.

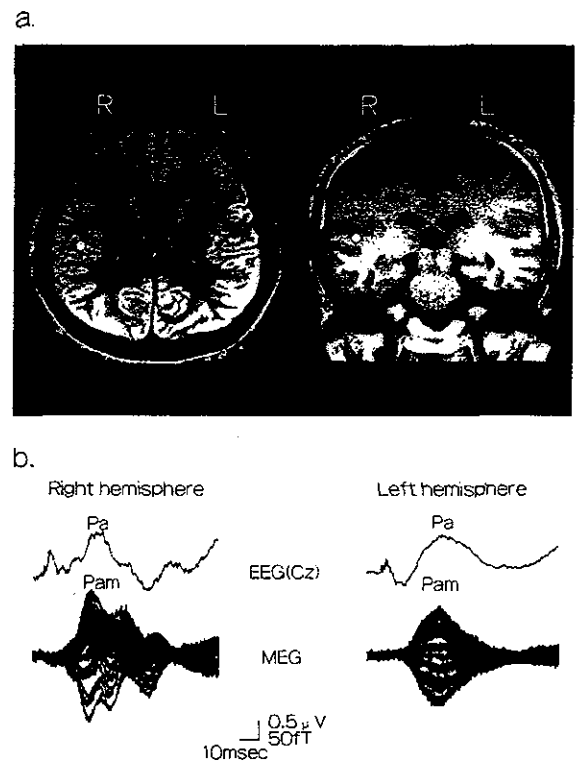

Fig. 1. (a) Superimposition of the ECD on the auditory cortex of the brain MRI scan. A white circle indicates the localization of the ECD. (b) Typical simultaneous recordings of AMLRs and MLAEFs in a normal subject, a 25-year-old male. Right- and left-hemisphere recordings were made with contralateral stimulation.

RESULTS

Controls

AMLRs and MLAEFs were recorded from 15 normal subjects for comparison. Typical recordings are shown in Fig. 1, in which the ECD is superimposed on the brain MRI scan. The ECD is localized in the auditory cortex in the right and left hemispheres. Control data are shown in Fig. 2a.

Patients

Left auditory cortex lesions. Nine patients who manifested sensory aphasia were studied. They were right-handed and had normal hearing. In most cases, their left primary and secondary auditory cortices had been damaged by their cerebrovascular accidents. Fig. 3 shows MLAEFs and the dipole localization fitted to the brain MRI scan for a typical patient, a 64-year-old male.

In Fig. 2b, the average latency and amplitude of the Pa in the AMLRs and the Pam in the MLAEFs from the right and left hemispheres are shown. There is no significant difference in the latency or amplitude of the Pa from the right and left hemispheres in the AMLRs. However, there is a significant difference in the r.m.s. amplitude of the Pam from the right and left hemispheres in MEG; there was no significant left–right difference in Pam latency.

Dipole locations of ECDs with relative coefficients > 0.98 were calculated. For the right hemisphere, eight of nine patients had coefficients > 0.98; only one of nine patients had no such correlation for the left hemisphere. Statistically, there was no difference between normal subjects and patients for the right hemisphere. A comparison between the left and right hemispheres among the patients, using paired t-tests, showed a significant difference in amplitude ($p < 0.05$) in eight patients. The other patient, whose relative coefficient was > 0.98, did not show significant differences between the right and left hemispheres.

Right auditory cortex lesion. Fig. 4 shows AMLRs and MLAEFs and the dipole localization fitted to the brain MRI scan for a typical patient, a 63-year-old male. The Pa of the AMLRs and MLAEFs was present from the left hemisphere in response to a right-ear stimulus. The Pam from the right hemisphere

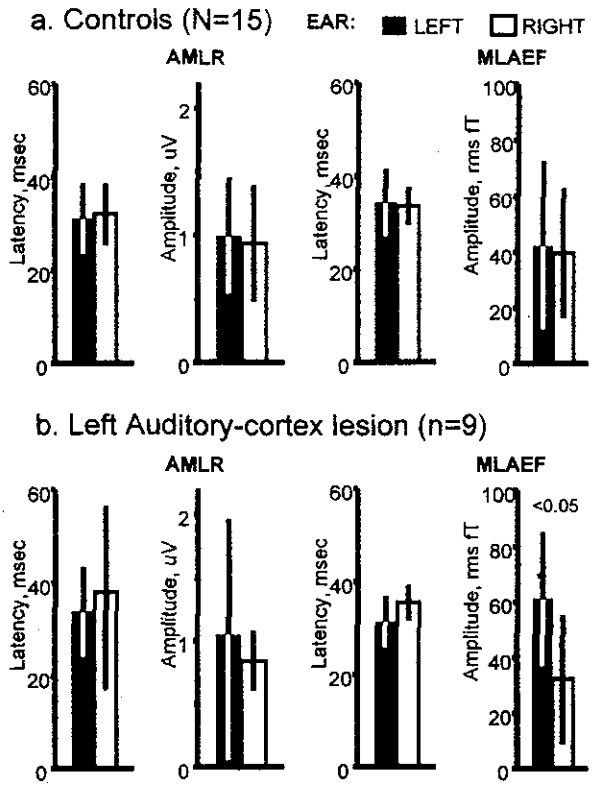

Fig. 2. (a) In data from 15 controls, there is no significant difference between the left and right hemispheres (right- and left-ear stimulation, respectively) in terms of the latency or amplitude of the AMLR or MLAEF. (b) In nine patients with left-hemisphere lesions, the MLAEF amplitude is significantly reduced for right-ear stimulation.

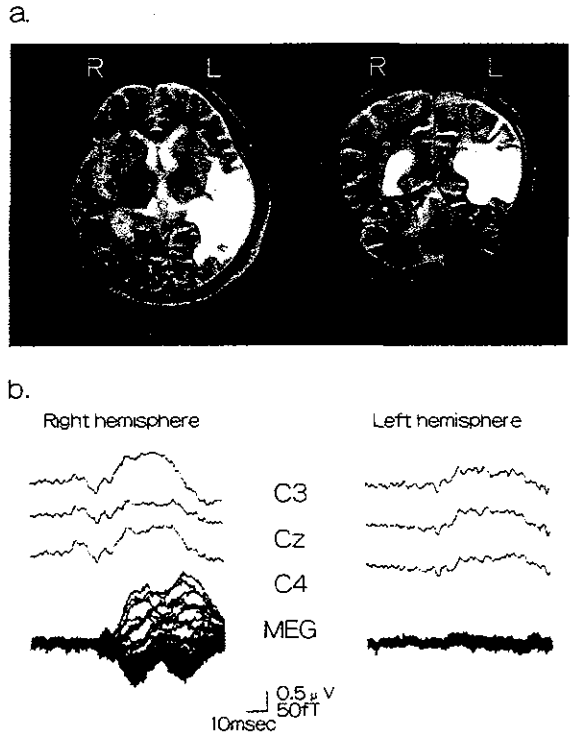

Fig. 3. A typical patient (64-year-old male) with a left auditory cortex lesion in the unilateral temporoparietal infarction. Brain MRI scans. AMLRs and MLAEFs are shown. The MLAEF is absent from the left hemisphere but is present from the right hemisphere. However, the AMLR persists bilaterally.

in response to a left stimulus was absent but the Pam from the left hemisphere was present in response to a right-ear stimulus. However, Pa of AMLR was present from both hemispheres.

DISCUSSION

This study demonstrates that the MLAEF generator is located in the auditory cortex because the ECD was localized to this area in patients with an undamaged auditory cortex but disappeared in patients with a damaged auditory cortex. The Pam of the MLAEF, which was evoked with the same latency as the Pa in the normal AMLR, was impaired or abolished in patients with lesions of the auditory cortex or its radiations. Pantev et al. (8) reported that clear Pam components of MLAEFs were recorded from the left hemisphere of each of 12 normal subjects when a short tone-burst stimulation was applied. As the specification of the SQUID gradiometers and the nature of the sound stimuli used differed between the studies, the results cannot be compared easily; however, the ECDs of the Pam were reported to be located in the left primary auditory cortex in the study of Pantev et al. (8). In our study, the ECDs recorded over the left hemisphere in normal subjects were localized in the primary auditory cortex. However, they were located slightly posterior to the estimated position reported by Pantev et al. (8) in normal subjects. This difference may be explained by recalling that the ECD is a hypothetical point source, which represents the center of activity (analogous to the center of gravity) of a source having some physical size. If the source includes both the anterior and posterior auditory cortices, an anterior lesion will cause the apparent center to move posteriorly. In our studies of the relationship between the damaged area and the position of the ECD, it is clear that most of the Pam disappears if the auditory cortex or auditory radiation is damaged, but that the Pam from the undamaged hemisphere persists. Our results suggest that at least part of the auditory cortex can be preserved, judging from the MLAEF analysis and the estimated position of the ECD.

For the reasons stated above, we conclude that the Pa and Pam do not reflect activities of identical generators. Woods et al. (4) speculated that the Pa amplitude is significantly influenced by the gradual

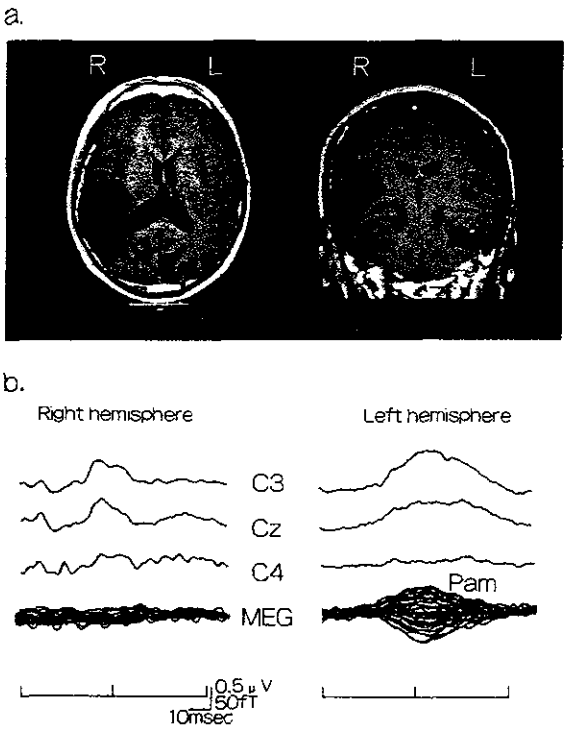

Fig. 4. A typical patient (63-year-old male) with a right auditory cortex lesion in the unilateral temporoparietal infarction. Brain MRI scans. AMLRs and MLAEFs are shown. The MLAEF is absent from the right hemisphere but the Pa is present from both hemispheres.

degeneration or denervation of subcortical structures, such as thalamic projection nuclei, and that this may explain the inconsistency in the presence of the Pa among patients with auditory cortex lesions.

Whereas the Pa reflects activities of several regions, including both auditory cortices, the thalamus and the reticular formation, the Pam, in contrast, almost exclusively reflects the activity of the auditory cortex ipsilateral to the sensor. Therefore, when diagnostic imaging of the auditory cortex is possible, MLAEF analysis with the Pam component as the index is more appropriate than AMLR analysis for functional diagnosis of the auditory cortex.

CONCLUSION

Compared to the Pa component of the AMLR, the Pam of the MLAEF is substantially more sensitive to the activity of the auditory cortex ipsilateral to the magnetic sensor. The primary generator of the Pam in MLAEFs has been demonstrated to be the auditory cortex. However, the Pa of AMLRs is evoked only partly from the auditory cortex because it is evoked even in patients with unilateral auditory cortex lesions.

ACKNOWLEDGEMENTS

We thank Ms M. Nakamura for technical assistance and Ms H Miyazaki for word processing. Roger R. Marsh, PhD of The Children's Hospital of Philadelphia made many helpful comments.

REFERENCES

1. Kaga K, Hink RF, Shinoda Y. Evidence for a primary cortical origin of a middle latency auditory evoked potential in cats. Electroencephalogr Clin Neurophysiol 1980; 50: 254–66.
2. Kraus N, McGee T, Littman T, Nicol T. Reticular formation influences on primary and non-primary auditory pathways as reflected by the middle latency response. Brain Res 1992; 587: 186–94.
3. Kraus N, Özdamar Ö, Hier D, Stein L. Auditory middle latency responses (MLRs) in patients with cortical lesions. Electroencephalogr Clin Neurophysiol 1982; 54: 275–87.
4. Woods DL, Clayworth CC, Knight RT, Simpson GV, Naeser MA. Generators of middle-and long-latency auditory evoked potentials: implications from studies of patients with bitemporal lesions. Electroencephalogr Clin Neurophysiol 1987; 68: 132–48.
5. Ibanez V, Deiber MP, Fisher C. Middle latency auditory evoked potentials in cortical lesions. Criteria of interhemispheric asymmetry. Arch Neurol 1989; 46: 1325–32.
6. Pantev C, Lütkenhöner B, Hoke M, Lehnertz K. Comparison between simultaneously recorded auditory-evoked magnetic fields and potentials elicited by ipsilateral, contralateral and binaural tone burst stimulation. Audiology 1986; 25: 54–61.
7. Pantev C, Hoke M, Lehnertz K, Lütkenhöner B. Neuromagnetic evidence of an amplitopic organization of the human auditory cortex. Electroencephalogr Clin Neurophysiol 1989; 72: 225–31.
8. Pantev C, Bertrand O, Eulitz C, Verkindt C, Hampson S, Schuierer G, et al. Specific tonotopic organization of different areas of the human auditory cortex revealed by simultaneous magnetic and electric recordings. Electroencephalogr Clin Neurophysiol 1995; 94: 26–40.
9. Hall DA, Hart HC, Johnsrude IS. Relationships between human auditory cortical structure and function. Audiol Neurotol 2003; 8: 1–18.
10. Pelizzone M, Hari R, Makela JP, Huttunen J, Ahlfors S, Hamalainen M. Cortical origin of middle-latency auditory evoked responses in man. Neurosci Lett 1987; 82: 303–7.
11. Makela JP, Hamalainen M, Hari R, McEvoy L. Whole-head mapping of middle-latency auditory evoked magnetic fields. Electroencephalogr Clin Neurophysiol 1994; 92: 414–21.
12. Yoshiura T, Ueno S, Iramina K, Masuda K. Effects of stimulation side on human middle latency auditory evoked magnetic fields. Neurosci Lett 1994; 172: 159–62.
13. Kuriki S, Nogai T, Hirata Y. Cortical sources of middle latency responses of auditory evoked magnetic field. Hear Res 1995; 92: 47–51.

Submitted September 1, 2003; accepted September 11, 2003

Address for correspondence:
Kimitaka Kaga
Department of Otolaryngology
Graduate School of Medicine
University of Tokyo
7-3-1 Hongo, Bunkyo-ku
Tokyo 113-8655
Japan
Tel.: +81 3 5800 8665
Fax: +81 3 3814 9486
E-mail: kimikaga-tky@umin.ac.jp

International Journal of Pediatric Otorhinolaryngology (2004) 68, 1115–1119

ELSEVIER

International Journal of Pediatric Otorhinolaryngology

www.elsevier.com/locate/ijporl

CASE REPORT

Hearing evaluation in two sisters with a T8993G point mutation of mitochondrial DNA

Yuki Sakai[a,b,*], Kimitaka Kaga[a,b], Kazuo Kodama[b], Asako Higuchi[c], Junko Miyamoto[c]

[a] *Department of Otolaryngology, School of Medicine, University of Tokyo, 7-3-1, Hongo, Bunkyo-ku, 113-8655 Tokyo, Japan*
[b] *National Center for Children's Rehabilitation, 1-1-10, Komone, Itabashi-ku, 173-0037 Tokyo, Japan*
[c] *Department of Pediatrics, Kiyose Children's Hospital, 1-3-1, Umezono, Kiyose-shi, 204-8567 Tokyo, Japan*

Received 10 September 2003; received in revised form 16 March 2004; accepted 18 March 2004

KEYWORDS
A T8993G point mutation of mitochondrial DNA;
Leigh's syndrome;
Neurogenic muscle weakness, ataxia, and retinitis pigmentosa (NARP);
Sensorineural hearing loss;
Auditory brainstem responses

Summary We report on two sisters with a T8993G point mutation of mitochondrial DNA, and their hearing evaluation. Considering auditory function, hearing in the elder sister remains almost normal. However, in the younger sister, the auditory brainstem response (ABR) threshold has fluctuated remarkably during a 3-year follow-up. The threshold changes of ABR in the younger sister suggest that her hearing problems may well be caused by both cochlear nerves and retrocochlear lesions. Our experience is clinically important because there have been only a few reports on hearing evaluation in patients with a T8993G point mutation of mitochondrial DNA.

1. Introduction

Mitochondrial encephalomyopathies are clinically heterogeneous disorders that can affect skeletal muscle and/or the central nervous system. Hearing loss caused by an inherited mitochondrial mutation has been described and is characterized by a maternal inheritance pattern [1]. In the most frequently encountered syndromes, such as the myoclonic epilepsia with red ragged fibers (MERRF), mitochondrial encephalopathy with lactic acid stroke-like episodes (MELAS), and Kearns–Sayre syndrome (KSS), 30–50% of patients exhibit a hearing loss [2]. Various mitochondrial mutations have been recognized to cause non-syndromal hearing loss. For example, an A1555G substitution in 12S ribosomal RNA in the mitochondrial genome together with exposure to an otherwise non-toxic aminoglicoside antibiotic or an additional genetic factor can lead to hearing impairment [3]. Similarly, an A3243G point mutation in the $tRNA^{Leu}$ gene has been associated with diabetes mellitus and sensorineural hearing loss [4]. Regarding mutations affecting the $tRNA^{(Ser)(UCN)}$ gene in mitochondria, four different mutations have been identified, all of which

*Corresponding author. Present address: ATORU MASAGO 701, 1-35-27 Hongo, Bunkyo-ku, 113-0033 Tokyo, Japan.
Tel.: +81-3-5800-8665; fax: +81-3-3814-9486.
E-mail address: xxxsakai@livedoor.com (Y. Sakai).

0165-5876/$ – see front matter © 2004 Elsevier Ireland Ltd. All rights reserved.
doi:10.1016/j.ijporl.2004.03.015

causes sensorineural hearing loss [2]. The A7445G point mutation in the $tRNA^{(Ser)(UCN)}$ gene causes not only hearing loss but palmoplantar keratoderma as well [5]. Hearing loss, ataxia and myoclonus were present in a large kindred from Sicily with a heteroplasmic C7472 nucleotide insertion in the same gene [6]. A mentally retarded 26-year-old woman with a T7512C mutation in this gene who suffered from myoclonic seizures, muscle atrophy weakness, and hearing disturbances lasting for a few seconds has also been documented [7]. In addition to these mutations, the T7510C mutation was described in a small family of 10 individuals with non-syndromal sensorineural hearing impairment [8]. In patients with these mutations, the age of hearing loss onset ranges from congenital to adulthood, and the severity ranges from mild to severe [2]. To our knowledge, descriptions of hearing loss in patients with a T8993G point mutation of mitochondrial DNA are only a few. A T8993G point mutation was first reported by Holt et al. [9] to cause a variable combination of developmental delay, retinitis pigmentosa, dementia, seizure, ataxia, and proximal neurogenic muscle weakness. They examined blood and muscle from patients to determine whether a correlation existed between clinical severity and the amount of mutant mitochondrial DNA. Following this report, Tatuch et al. [10] described how a heteroplasmic mitochondrial DNA mutation at T8993G could cause Leigh's syndrome when the percentage of abnormal mitochondrial DNA was high. This association was confirmed by other workers [11,12]. In these reports, hearing loss in the patients was not described. We investigated hearing in two sisters who have Leigh's syndrome with a T8993G point mutation of mitochondrial DNA using auditory brainstem response (ABR) and we found ABR abnormalities in the younger sister.

2. Case report

Two sisters (currently 11- and 4-year-old) experienced repeated epileptic seizures several months after birth. They were examined in Kiyose Children's Hospital. Brain CT scanning showed bilateral low density areas in the basal ganglia and the posterior limb of the internal capsule. They were suspected of having Leigh's syndrome associated with a mitochondrial disease. In the clinical findings, lactate and pyruvate levels were high in the spinal fluid in the elder sister, and those acids were high in both the serum and spinal fluid in the younger sister. They had neurogenic muscle weakness, ataxia, and retinitis pigmentosa (NARP) as well as epileptic seizures, and were also mentally

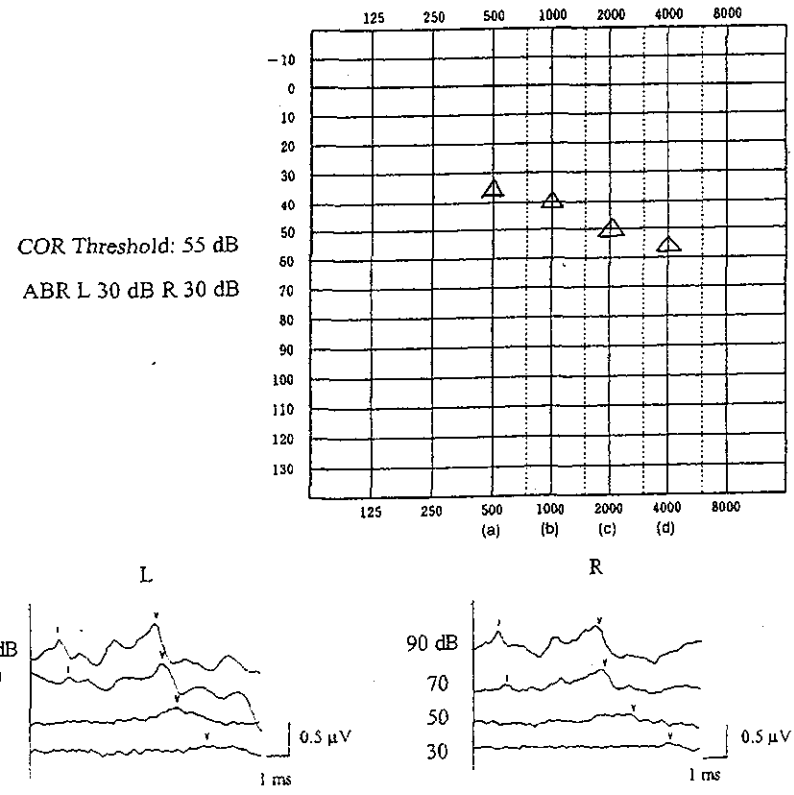

Fig. 1 COR and ABR at 8 years of age in the elder sister (L: left ear, R: right ear).

retarded. No abnormalities were found in glucose tolerance. They were diagnosed as having a T8993G point mutation of mitochondrial DNA based on the results of genetic evaluation. Their mother had the same mutation, but was asymptomatic. She had no hearing loss. Because these sisters had poor response to sound, they were referred to our hospital for hearing evaluation when the elder sister was 8 years old and the younger sister was 8 months.

2.1. Elder sister

The otoscopic findings revealed no abnormalities. Fig. 1 shows the results of conditioned response audiometry (COR) and ABR in the elder sister when she was 8 years old. The COR threshold was slightly elevated (55 dB). In the first ABR measurement, the threshold was 30 dB in both ears. Peak latency of wave I and wave V, and peak interval of wave I–V at 90 dB were not delayed (Table 1). The COR threshold has not changed since that time.

2.2. Younger sister

Fig. 2 shows the measurement of ABR in the younger sister at 8 months, 1 year, 1.5 years, and 3 years of age. The otoscopic findings showed no abnormalities. At 8 months, the threshold was 20 dB in both ears. However, the threshold was elevated to 90 dB in the left ear and 70 dB in the right at 1 year of age. The threshold had improved in the younger sister at 1 year and 5 months of age to 30 dB in both ears. However, it deteriorated to 70 dB in the left ear and 90 dB when she was 3 years old, with low

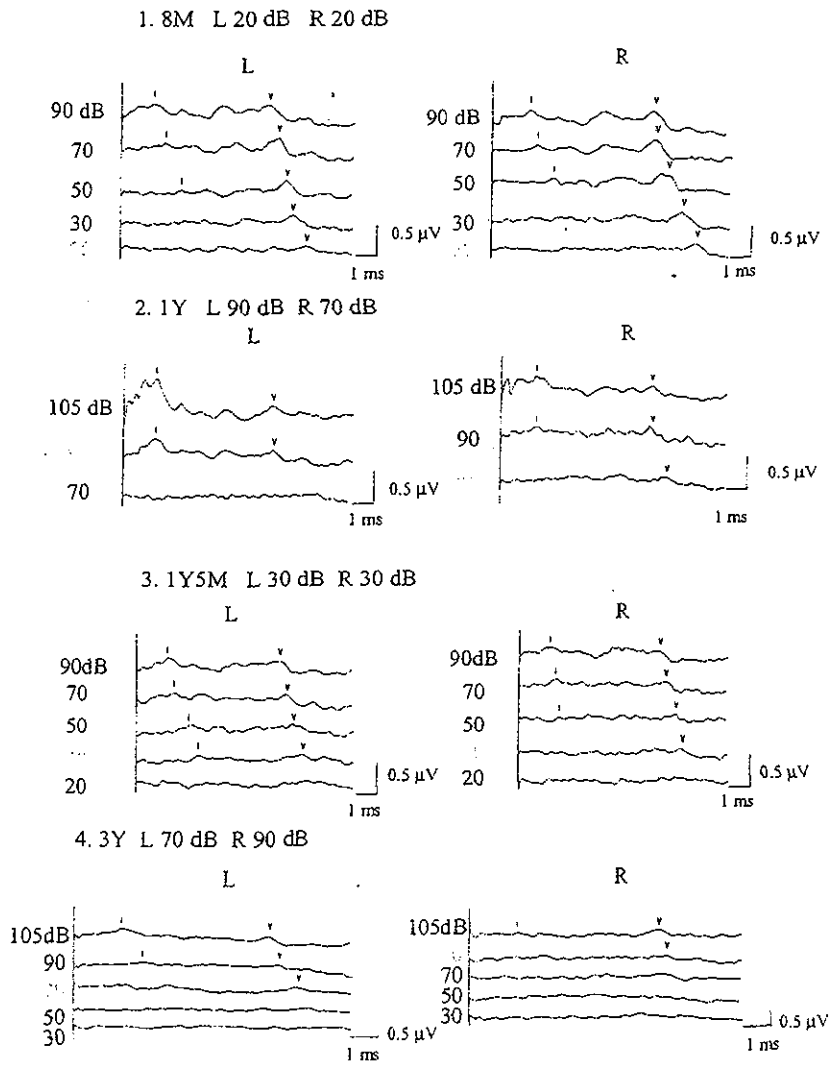

Fig. 2 The measurement of ABR in the younger sister at 8 months, 1 year, 1.5 years and 3 years of age (M: months of age, Y: years of age, L: left ear, R: right ear).

Table 1 Peak latency of wave I and wave V, and peak interval of wave I–V at 90 dB in ABR

	Age	Wave I peak latency (ms)	Wave V peak latency (ms)	Wave I–V peak interval (ms)
Elder sister	8 Y	R 1.35, L 1.25 (1.39 ± 0.07)	R 5.49, L 5.37 (5.42 ± 0.25)	R 4.14, L 4.12 (4.03 ± 0.31)
Younger sister	8 M	R 1.46, L 1.58 (1.42 ± 0.06)	R 6.59, L 6.38 (5.94 ± 0.20)	R 5.13, L 4.80 (4.52 ± 0.13)
	1 Y	R 1.43, L 1.50 (1.41 ± 0.09)	R 6.51, L 6.42 (5.92 ± 0.23)	R 5.08, L 4.92 (4.51 ± 0.19)
	1.5 Y	R 1.39, L 1.48 (1.41 ± 0.09)	R 6.87, L 6.61 (5.92 ± 0.23)	R 5.48, L 5.13 (4.51 ± 0.19)
	3 Y	R (–), L 1.47 (1.45 ± 0.04)	R 6.51, L 6.25 (5.66 ± 0.08)	R (–), L 4.78 (4.21 ± 0.11)

Mean and S.D. of the control data are shown under each result, M: months of age, Y: years of age).

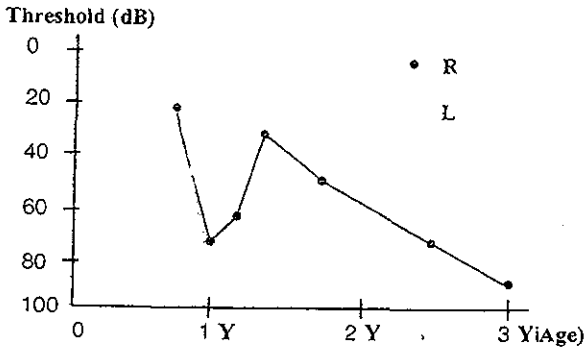

Fig. 3 A line graph of the threshold changes in ABR from 8 months to 3 years of age in the younger sister. The vertical axis is the threshold and the horizontal axis is her age (Y: years of age).

amplitude. Her COR was uncertain. In each recording of the ABR, peak latency of wave I and wave V, and peak interval of wave I–V at 90 dB were delayed compared with those from our age-matched control data (Table 1). A distortion products otoacousitic emissions (DPOAE) study revealed normal DPOAE.

By the age of 3 years, we had recorded ABR seven times in the younger sister. Fig. 3 shows a line graph of the threshold changes in her ABR. The threshold was normal at 8 months, but it had deteriorated markedly by the time she reached 1 year of age, and afterward it improved rapidly, however, subsequently it gradually worsened.

3. Discussion

Hearing in the elder sister is almost normal based on the results of the COR and ABR measurement. In the younger sister, she had no abnormalities at delivery and a few months after birth. Considering the results of her DPOAE tests, her bilateral inner ears are almost normal. However, the amplitude of the ABR at 3 year of age was low. These findings of DPOAE and ABR indicate that the responsible lesion causing hearing loss in the younger sister might involve the cochlear nerves. Moreover, the peak latency of wave I and wave V and the peak interval of wave I–V at 90 dB are markedly delayed. These findings demonstrate that retrocochlear problems exist in her hearing loss. Kaga et al. [13] reported auditory brainstem responses in Leigh's syndrome. They studied the lesions in patients with Leigh's syndrome using brain CT and ABRs. Abnormalities of ABRs were detected in the early stages of the disease in all patients but ABR configurations differed in the lesion. In some patients with the cortical form of Leigh's syndrome, the configuration became nearly flat with the passage of time. That was similar to our observations. Yoshinaga et al. [14] noted an abnormality in the ABR from the early stages in a child with a T8993G point mutation of mitochondrial DNA. III–V interpeak latency of the child was prolonged, and wave V amplitude was low at the age of 7 months. After that, the auditory response deteriorated, and loss of all components was demonstrated at the age of 3 years 5 months. This result was the same as ours. It was thought that the retrocochlear problems in our younger patient must be related to Leigh's syndrome. In regards to heteroplasmy, Yoshinaga et al. [14] described the clinical course of patients with a T8993G point mutation will change according to proportionality of mutant and wild type mitochondrial DNA and to what organs are affected most, while several reports emphasized the degree of hearing loss was not clearly correlated with the amount of the mutant mitochondrial DNA, indicating that other, yet unidentified factors are responsible in other mitochondrial disorders [2,15,16]. Therefore, the definitive reason for the fluctuating hearing loss in our case remains unknown. In terms of auditory behavior, the elder sister can locate sound sources easily and can engage in limited communication with others through gestures. The younger sister responded to sounds better when her ABR threshold improved. We thought that it would be difficult to fit the younger sister with a hearing aid because of the fluctuation in the threshold and her mental retardation.

References

[1] N. Fischel-Ghodsian, Mitochondrial mutations and hearing loss-paradigm for mitochondrial genetics, Am. J. Hum. Genet. 62 (1998) 15–19.

[2] W.R.J. Cremers Cor, R.J.H. Smith (Eds.), Genetic Hearing Impairment Adv. Otolaryngol., vol. 61, Basel, Kerger, 2002, pp. 172–183.

[3] T.R. Prezant, J.V. Agapian, M.C. Bohlman, Mitochondrial ribosomal RNA mutation associated with both antibiotic-induced on non-syndromic deafness, Nature Genet. 4 (1993) 289–294.

[4] S. Manouvrier, A. Rotig, G. Hannebique, Point mutation of the mitochondrial $tRNA^{Leu}$gene (A3243G) in maternally inherited hypertrophic cardiomyopathy, diabetes mellitus, renal failure, and sensorineural deafness, J. Med. Genet. 32 (1995) 654–656.

[5] F.M. Reid, G.A. Vernham, H.T. Jacobs, Complete mt DNA sequence of a patients in a maternal pedigree with sensorineural deafness, Hum. Mol. Genet. 3 (1994) 1435–1436.

[6] V. Tiranti, P. Chariot, Carella, Hum. Mol. Genet 4 (1995) 1421–1427.

[7] M. Nakamura, S. Nakano, Y.I. Gato, A novel point mutation in the mitochondrial $tRNA^{(Ser)(UCN)}$gene detected in a family with MERRF/MELAS overlap syndrome, Biochem. Biophys. Res. Commun. 214 (1995) 86–93.

[8] T. Hutchin, M.J. Parker, I.D. Young, A novel mutation in the mitochondrial $tRNA^{(Ser)(UCN)}$gene in a family with non-syndromal sensorineural hearing impairment, J. Med. Genet. 37 (2000) 692–694.

[9] I.J. Holt, A.E. Harding, R.K.H. Petty, A new mitochondrial disease associated with mitochondrial DNA heteroplasmy, Am. J. Hum. Genet. 46 (1990) 428–433.

[10] Y. Tatuch, J. Christodoulou, A. Feigenbaum, Heteroplasmic mtDNA mutation (T → G) at 8993 can cause Leigh disease when the percentage of abnormal mtDNA is high, Am. J. Hum. Genet. 50 (1992) 852–858.

[11] F.M. Santorelli, S. Shanske, A. Macaya, The mutation at nt 8993 of mitochondrial DNA is a common cause of Leigh's syndrome, Ann. Neurol. 34 (6) (1993) 827–834.

[12] J.M. Soffner, P.M. Fernhoff, N.S. Krawiecki, Subacute necrotizing encephalopathy: oxidative phosphorylation defects and the ATPase 6 point mutation, Neurol. 42 (1992) 2168–2174.

[13] M. Kaga, H. Naitoh, K. Nihei, Auditory brainstem response in Leigh's syndrome, Acta Paediatr. Jpn. 29 (1987) 254–260.

[14] H. Yoshinaga, T. Ogino, S. Ohtahara, A T-to-G mutation at nucleotide pair 8993 in mitochondrial DNA in a patient with Leigh's syndrome, J. Child Neurol. 8 (2) (1993) 129–133.

[15] F. Reid, A. Rovio, I.J. Holt, Molecular phenotype of a human lynphoblastoid cell line homoplasmic for the np7445 deafness-associated mitochondrial mutation, Hum. Mol. Genet. 6 (1997) 443–449.

[16] R.J.H. Ensink, H.A.M. Marres, C.W.R.J. Cremers, Early-onset maternal inherited hearing loss with late-onset neurological symptoms present in a three-generation Dutch family, in: Proceedings of the Second Workshop European Working Group on Genetics of Hearing Impairment, Milan, October 1996.

Acta Otolaryngol 2004; Suppl 553: 23–27

Taylor&Francis healthsciences

Actions of Subtype-specific Purinergic Ligands on Rat Spiral Ganglion Neurons

KEN ITO[1], SHINICHI IWASAKI[1], KENJI KONDO[1], DIDIER DULON[2] and KIMITAKA KAGA[1]

From the [1]Department of Otolaryngology, Faculty of Medicine, University of Tokyo, Tokyo, Japan and [2]Laboratoire de Biologie Cellulaire et Moléculaire de l'Audition, INSERM EMI 99-27, Université de Bordeaux 2, Hôpital Pellegrin Bat PQR, Bordeaux, France

Ito K, Iwasaki S, Kondo K, Dulon D, Kaga K. *Actions of subtype-specific purinergic ligands on rat spiral ganglion neurons.* Acta Otolaryngol 2004; Suppl 553: 23–27.

In a previous study we showed that, in rat spiral ganglion neurons (SGNs), the adenosine 5′-triphosphate (ATP)-evoked currents were a combination of the activation of ionotropic receptors (the first fast current) and the activation of metabotropic receptors which secondarily opened non-selective cation channels. These two conductances imply the involvement of different receptor subtypes. In the present study, we tested three subtype-specific purinergic ligands: α, β-methylene ATP (α,β-meATP) for P2X receptors, uridine 5′-triphosphate (UTP) for P2Y receptors and 2′-3′-O-(4-benzoylbenzoyl) ATP (Bz-ATP) for P2Z ($P2X_7$) receptors. Application of 100 μM α,β-meATP did not trigger any significant change in membrane conductance, while the SGNs were responsive to ATP. Pressure application of UTP (100 μM, 1 s) evoked an inward current averaging 344±169 pA at a holding potential of −50 mV. The conductance developed after a latency averaging 1.5±0.6 s, took 4–6 s to peak and reversed slowly within 15–30 s. The current–voltage curve reversed near 0 mV, suggesting a non-selective cation conductance, like the second component of the ATP conductance. Bz-ATP evoked an inward current which developed without latency, was sustained during ligand application and was rapidly inactivated at the end of application: the same characteristics as the first component of the ATP-evoked current. The Bz-ATP conductance reversed around −10 mV, indicating also a non-selective cation conductance. These results suggest that, in SGNs, ATP acts via two different receptor subtypes, ionotropic P2Z receptors and metabotropic P2Y receptors, and that these two receptor subtypes can assume different physiological roles. *Key words: P2X, P2Y, P2Z, purinergic receptor, spiral ganglion neuron.*

INTRODUCTION

While glutamate is recognized as the principal neurotransmitter at the inner hair cell–spiral ganglion neuron (SGN) synapse, other neurochemicals, including adenosine 5′-triphosphate (ATP), have been proposed to act as neuromodulators at the efferent synapse on the SGNs (1). The existence of purinergic receptors on SGNs has been shown by autoradiography (2), in situ hybridization (3) and immunolocalization (4) techniques. These receptors were found to be physiologically functional as the result of in vivo (5) and in vitro (4, 6) studies. We recently reported (7) a depolarizing cation non-selective conductance evoked by ATP in rat SGNs. Figure 1 summarizes the typical characteristics of this conductance. Brief application of ATP evoked a reversible inward current (Fig. 1a). The current evoked by ATP displayed two components: a first fast component without latency and a second slow component with a latency of ≈1 s. The second component was larger in amplitude, took 3–4 s to peak and reversed slowly within 15–30 s. The two components of the purinergic response could be easily separated and identified using a very brief application of ATP. Analysis of the current–voltage (I–V) relationship of this second component indicated a large increase in membrane conductance during application of ATP (Fig. 1b). ATP-evoked currents displayed an inward rectification at negative potentials and were reversed near 0 mV, indicating the activation of a non-selective cation conductance. These results suggested that the ATP-evoked currents were a combination of the activation of ionotropic receptors (the first fast current) and the activation of metabotropic receptors which secondarily opened non-selective cation channels. These two conductances imply the involvement of different receptor subtypes having different physiological roles. In the present study, we tested three subtype-specific purinergic ligands: α,β-methylene ATP (α,β-meATP) for P2X receptors, uridine 5′-triphosphate (UTP) for P2Y receptors and 2′-3′-O-(4-benzoylbenzoyl) ATP (Bz-ATP) for P2Z ($P2X_7$) receptors (8).

MATERIAL AND METHODS

Preparation of SGNs

Detailed procedures for freshly isolating SGNs have been published elsewhere (9). Briefly, rats (3–7 days old) were deeply anesthetized with an i.p. injection of 0.1–0.2 ml of a solution consisting of 1 volume of 50 mg/ml ketamine and 1 volume of 2% xylazine, and then decapitated. Cochleae were extracted from the temporal bone and bathed in Dulbecco's phosphate-buffered saline containing (mM): NaCl, 136.9; Na_2HPO_4, 6.5; KCl, 2.7; KH_2PO_4, 1.5; $CaCl_2$, 0.9; and $MgCl_2$, 0.5, with the pH adjusted to 7.3. The shell was opened and the stria vascularis and the organ of Corti were removed. Spiral ganglions were extracted from the spiral lamina of the two basal turns. The SGNs were isolated by mechanical dissociation following enzymatic treatment with trypsin (type III; 100 μg/ml, 37°C, 30 min) on glass coverslips (diameter 30 mm, thickness 0.13–0.17 mm) sealed in the middle of

 ISSN 0365-5237

DOI 10.1080/03655230410017616

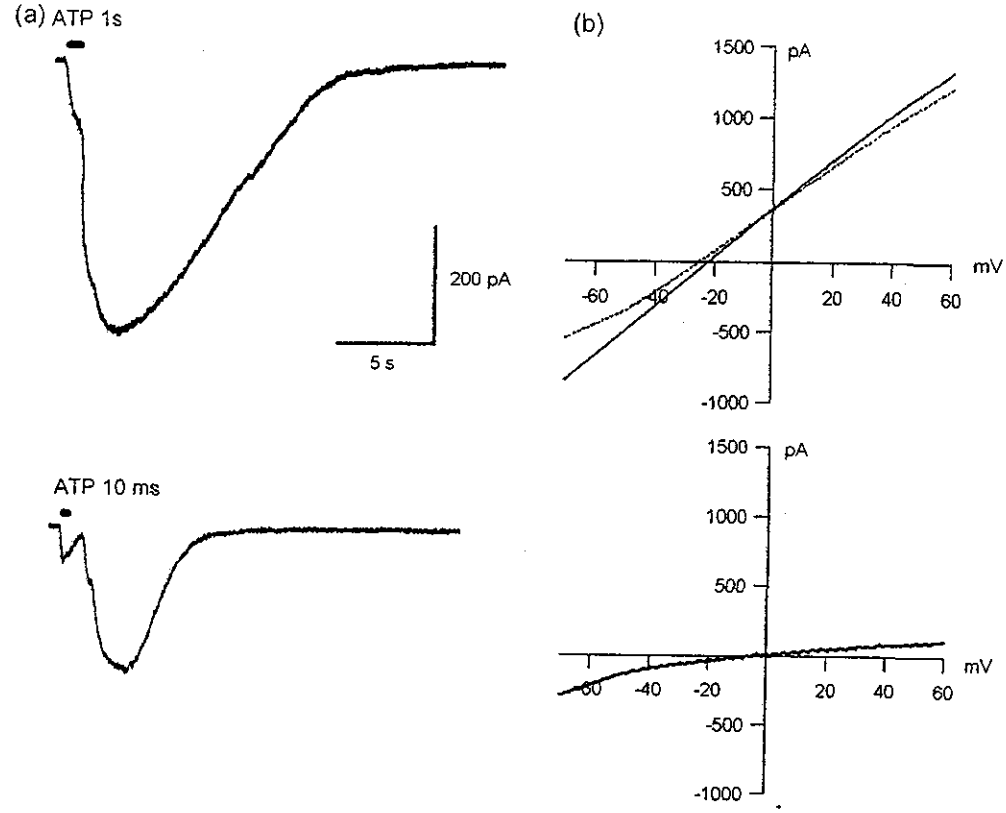

Fig. 1. (a) Top trace: a brief application (1 s) of ATP (100 μM) evoked a reversible inward current under the voltage-clamp condition at −50 mV. Bottom trace: the two purinergic components could be isolated in the time domain by using a very short (10 ms) application of ATP (100 μM). The same SGN was held at −50 mV. (b) Example of a typical I–V relationship obtained using the ramp protocol in an SGN stimulated with 100 μM ATP. Upper: solid and dotted traces represent the currents during and without activation of the second component of the purinergic (ATP) conductance, respectively. Lower: the purinergic current obtained by subtraction.

perforated Petri dishes (35 mm diameter; Nunc). Before starting the experiments, SGNs were left to rest for at least 2 h at room temperature. Identification of SGNs under a microscope was facilitated by their shape and grouping and by the remnants of dendrites or axons (9). Our results were obtained essentially from type I SGNs, which represented >95% of the cells in our preparation. Type I SGNs from newborn rats could be distinguished from the rare type II SGNs by their larger size and the presence of a soft, thin myelin shield.

Electrophysiological recordings

Recordings on SGNs were performed with the conventional whole-cell patch clamp configuration, using an Axopatch-1D amplifier (Axon Instruments, Foster City, CA). Electrodes were pulled from borosilicate glass capillaries (GC150TF-10; Clark Electromedical, UK). The internal solution consisted of (mM): KCl, 158; KOH, 3.5; $MgCl_2$, 2.0; ethylene glycol tetraacetic acid, 1.1; and 4-(2-hydroxyethyl)-1-piperazinethansulfonic acid, 5.0, with the pH adjusted to 7.2 and the osmolality adjusted to 300 mOsm. Axotape and pCLAMP software (Axon Instruments) and IGOR Pro software (Wavemetrics Inc., Lake Oswego, OR) were used for data collection and analysis. Junction potentials were set to zero immediately before gigaseal formation. Electrode resistance ranged from 3 to 6 MΩ. The electrode capacitance and series resistance were not corrected at the time of experimentation. I–V relationships were obtained from voltage ramps (−80 mV to +70 mV, 900 ms) and corrected for series resistance-induced voltage errors. The ramp protocol started from a holding potential of −50 mV, jumped to −80 mV for 20 ms and then swept linearly to +70 mV over a 900-ms period. In order to measure the I–V relationship during agonist stimulation, we started the ramp protocol at the peak current.

Drug application

Test solutions were applied to SGNs using a Picospritzer puffer system (Picospritzer II; General Valve, Fairfield, NJ) as previously described (10). Puff pipettes were pulled similarly to the recording patch clamp pipettes. The tips of the pipettes were placed ≈20–40 μm from the SGNs. The delay for drugs to

reach the cell ranged from 20 to 50 ms (10). When repetitive applications of drugs were made to the same SGN, we waited for at least 2 min between applications in order to reduce desensitization.

All experiments were performed at room temperature (20–22°C). All reagents were purchased from Sigma Chemical Company. The data are expressed as mean ± SD unless specifically noted otherwise.

RESULTS

Responses to the P2X ligand

Application of 100 μM α,β-meATP did not trigger any significant change in membrane conductance, while the SGNs were responsive to ATP ($n = 5$; Fig. 2).

Responses to the P2Y ligand

Under the whole-cell voltage clamp condition, pressure application of UTP (100 μM, 1 s) evoked an inward current in 71% of tested SGNs ($n = 17$; Fig. 3a), averaging 344 ± 169 pA at a holding potential (Vh) of −50 mV. The conductance developed after a latency averaging 1.5 ± 0.6 s, took 4–6 s to peak and reversed slowly within 15–30 s. Analysis of the I–V relationship of the UTP response, tested with a voltage-ramp protocol, indicated a large increase in membrane conductance (Fig. 3b). The I–V curve showed inward rectification at negative membrane potentials and was reversed at 3.3 ± 8.6 mV ($n = 4$). These results demonstrated that UTP activated a non-selective cation conductance, like the second component of the ATP conductance. The long delay between ligand application and activation of conductance confirms the involvement of metabotropic processes evoked by P2Y receptors.

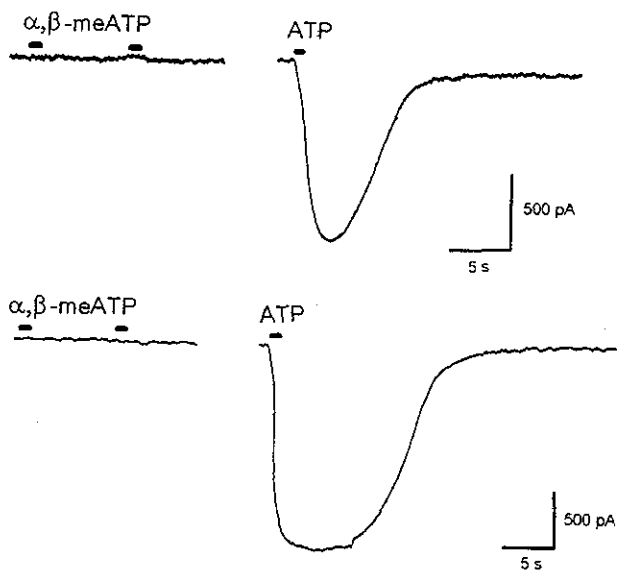

Fig. 2. Application of α,β-meATP (100 μM, 1 s) did not evoke a current while the SGNs were responsive to ATP (Vh = −50 mV). Two examples are shown.

Responses to the P2Z ligand

Under the whole-cell voltage clamp condition, pressure application of Bz-ATP (100 μM, 1 s) evoked an inward current in 69% of tested SGNs ($n = 16$; Fig. 4a). The Bz-ATP current developed without latency, was sustained during Bz-ATP application and was rapidly inactivated at the end of the ligand application: the same characteristics as the first component of the ATP-evoked current [see Fig. 5a of our previous paper (7)]. The I–V relationship of the Bz-ATP response, measured during prolonged ligand application, also indicated an increase in membrane conductance (Fig. 4b). The Bz-ATP conductance reversed at −11.7 ± 13.0 mV ($n = 4$), indicating also a non-selective cation conductance, but with a smaller permeability than that of the ATP-evoked second component and the UTP conductance.

DISCUSSION

In summary, the present results showed that Bz-ATP, a P2Z ligand, and UTP, a P2Y ligand, evoked current responses very similar to the first and second components of the ATP response, respectively. No measurable responses occurred with α,β-meATP, a P2X ligand. In SGNs, P2Y receptors are supposed to mobilize intracellular calcium (6) and to open, via metabotropic processes, the large cation non-selective channels which have been shown to be shared by various ligands (7, 11). P2Z receptors are known to increase cell permeability by opening large cation non-selective channels (8), which is consistent with our present results. Although P2Z receptors have been demonstrated in the central nervous system (12), this is the first report of functional P2Z receptors in SGNs. Regarding P2X receptors in rat SGNs, there remains scope for their possible involvement, as α,β-meATP has been shown to be inactive with certain subtypes of P2X receptors, e.g. $P2X_2$, $P2X_5$ and $P2X_6$, in certain cell types (8). However, there is no more perfectly subtype-specific ligand. For example, 2-methylthio ATP is a more potent ligand for P2X receptors but also interacts with P2Y receptors. Involvement of different types of receptors can suggest different physiological roles. P2Z ($P2X_7$) receptors were initially considered to cause cell lysis by increasing cell permeability but were subsequently postulated to mediate fast synaptic transmission or modulation (12). In contrast, P2Y receptors may regulate neuronal excitability more slowly by changing the resting potential. Moreover, P2Y receptors may affect neuronal survival by increasing the intracellular calcium

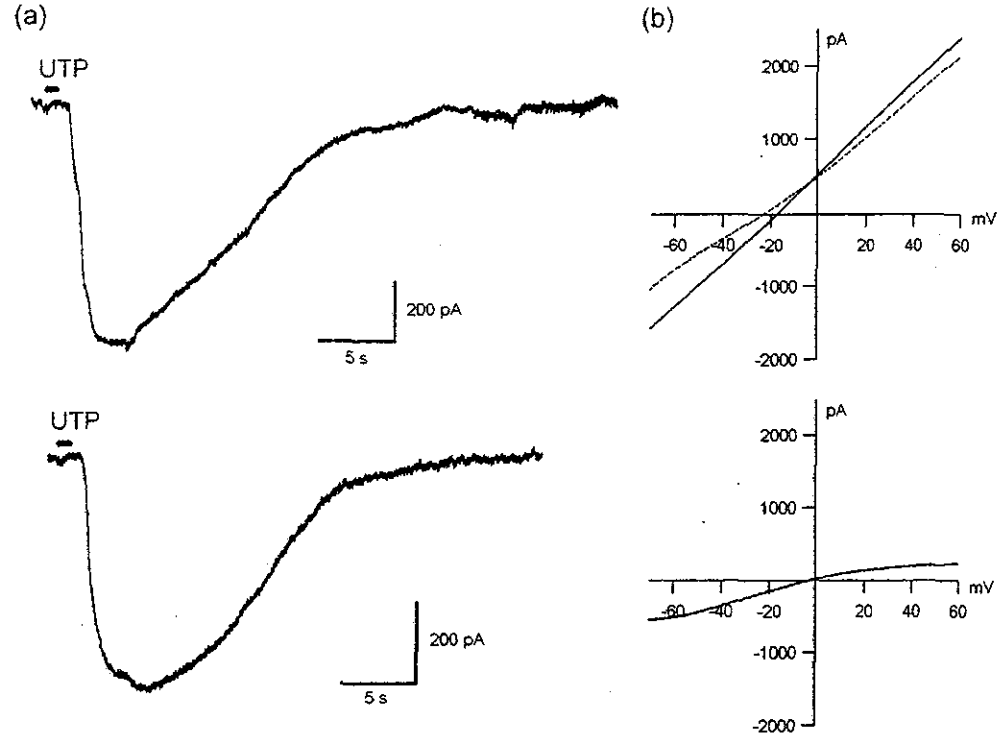

Fig. 3. (a) Brief application (1 s) of UTP (100 μM) evoked a reversible inward current under the voltage-clamp condition at −50 mV. The conductance was evoked with a latency of ≈1.5 s, i.e. it developed after application of the ligand ceased. Two examples are shown. (b) Example of a typical I–V relationship obtained using the ramp protocol in an SGN stimulated with 100 μM UTP. Upper: solid and dotted traces represent the currents during and without activation of the UTP conductance, respectively. Lower: the UTP current obtained by subtraction.

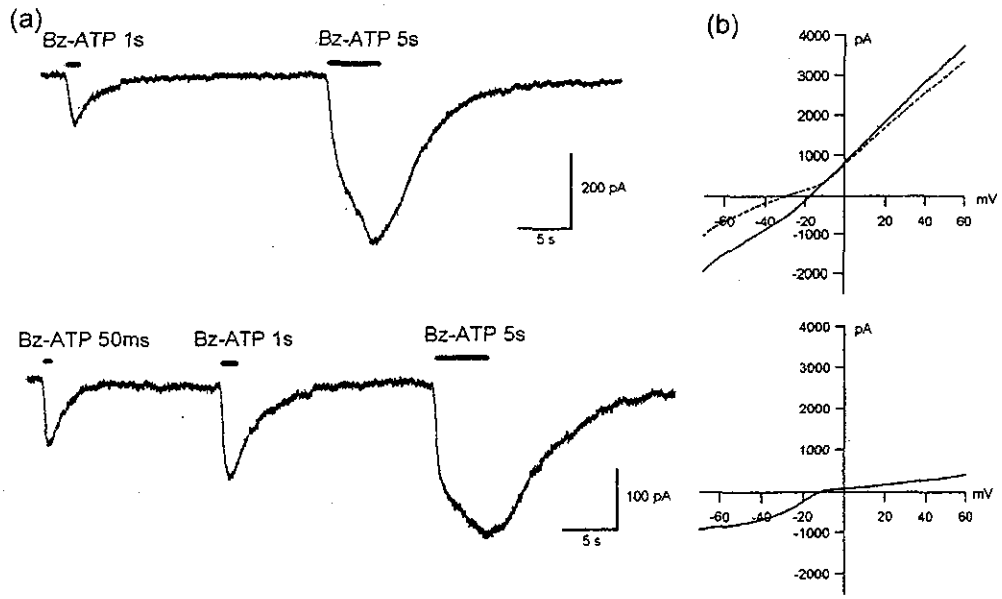

Fig. 4. (a) Examples of Bz-ATP-evoked conductance. The current developed without latency, was sustained during ligand application (100 μM Bz-ATP) and was inactivated rapidly after application had ceased. The SGN was held at −50 mV. (b) Example of a typical I–V relationship obtained using the ramp protocol in an SGN stimulated with 100 μM Bz-ATP. Upper: solid and dotted traces represent the currents during and without activation of the Bz-ATP conductance, respectively. Lower: the Bz-ATP current obtained by subtraction.

concentration (13). More intensive in vivo studies are required in order to determine precisely the physiological effects of these purinergic receptors on SGNs.

ACKNOWLEDGEMENT

Part of this work was supported by the Canon Foundation Europe (Leiden, The Netherlands).

REFERENCES

1. Eybalin M. Neurotransmitters and neuromodulators of the mammalian cochlea. Physiol Rev 1993; 73: 309–73.
2. Mockett BG, Bo X, Housley GD, Thorne PR, Burnstock G. Autoradiographic labelling of P2 purinoceptors in the guinea-pig cochlea. Hear Res 1995; 84: 177–93.
3. Housley GD, Luo L, Ryan AF. Localization of mRNA encoding the P2X2 receptor subunit of the adenosine 5′-triphosphate-gated ion channel in the adult and developing rat inner ear by in situ hybridization. J Comp Neurol 1998; 393: 403–14.
4. Salih SG, Housley GD, Raybould NP, Thorne PR. ATP-gated ion channel expression in primary auditory neurones. Neuroreport 1999; 10: 2579–86.
5. Chen C, Skelett RA, Fallon M, Bobbin RP. Additional pharmacological evidence that endogenous ATP modulates cochlear mechanics. Hear Res 1998; 118: 47–61.
6. Cho H, Harada N, Yamashita T. Extracellular ATP-induced $Ca2^+$ mobilization of type I spiral ganglion cells from the guinea pig cochlea. Acta Otolaryngol (Stockh) 1997; 117: 545–52.
7. Ito K, Dulon D. Nonselective cation conductance activated by muscarinic and purinergic receptors in rat spiral ganglion neurons. Am J Physiol Cell Physiol 2002; 282: C1121–35.
8. Ralevic V, Burnstock G. Receptors for purines and pyrimidines. Pharmacol Rev 1998; 50: 413–92.
9. Rome C, Luo D, Dulon D. Muscarinic receptor-mediated calcium signaling in spiral ganglion neurons of the mammalian cochlea. Brain Res 1999; 846: 196–203.
10. Blanchet C, Erósteguí C, Sugasawa M, Dulon D. Acetylcholine-induced potassium current of guinea-pig outer hair cells: its dependence on a calcium influx through nicotinic-like receptors. J Neurosci 1996; 16: 2574–84.
11. Ito K, Rome C, Bouleau Y, Dulon D. Substance P mobilizes intracellular calcium and activates a nonselective cation conductance in rat spiral ganglion neurons. Eur J Neurosci 2002; 16: 2095–102.
12. Surprenant A, Rassendren F, Kawashima E, North RA, Buell G. The cytolytic P2Z receptor for extracellular ATP identified as a P2X receptor (P2X7). Science 1996; 272: 735–8.
13. Hegarty JL, Kay AR, Green SH. Trophic support of cultured spiral ganglion neurons by depolarization exceeds and is additive with that by neurotrophins or cAMP and requires elevation of [Ca2+]i within a set range. J Neurosci 1997; 17: 1959–70.

Address for correspondence:
Ken Ito, MD
Department of Otolaryngology
Faculty of Medicine
University of Tokyo
7-3-1 Hongo, Bunkyo-ku
Tokyo 113-8655
Japan
Tel.: +81 3 5800 8665
Fax: +81 3 3814 9486
E-mail: itoken-tky@umin.ac.jp

Cortical mapping of auditory-evoked offset responses in rats

Hirokazu Takahashi,[CA] Masayuki Nakao and Kimitaka Kaga[1]

Department of Engineering Synthesis, Graduate School of Engineering, The University of Tokyo, Tokyo, 113-8656, Japan; [1]Department of Otolaryngology, and Head and Neck Surgery, Graduate School of Medicine, The University of Tokyo, 7-3-1 Hongo, Bunkyo-ku, Tokyo, 113-8655, Japan

[CA]Corresponding Author: hiro@hnl.t.u-tokyo.ac.jp

Received 6 April 2004; accepted 17 May 2004

DOI: 10.1097/01.wnr.0000134848.63755.5c

We characterized the auditory-evoked offset responses of the rat auditory cortex by multiple-site surface microelectrode recording. Tone bursts served as test stimuli. Offset responses did not appear tonotopically, but at the fringe of tonotopic onset distributions. Offset amplitude was significantly sensitive to sound intensity, fall time at tone termination, and duration. These results suggest that offset responses are associated with inhibitory responses surrounding excitatory onset responses, and offset responses become large when inhibition becomes strong and long or terminates synchronously. Thus, the rebound after the inhibition in the presence of a stimulus is likely to be a major cause of offset responses in the auditory cortex. *NeuroReport* 15:1565–1569 © 2004 Lippincott Williams & Wilkins.

Key words: Auditory cortex; Auditory evoked potential; Duration tuning; Functional organization; Off neuron; Offset response; Rat; Surface microelectrode array

INTRODUCTION

Auditory-evoked offset responses that appear after the cessation of auditory stimuli under particular conditions have been described in auditory brain stem response (ABR) studies [1,2] and in MEG studies of the auditory cortex [3,4]. Many unit studies also found that 10–30% of auditory neurons selectively respond after the termination of stimuli, from the auditory nerve [5] through the brain stem pathway [6–14] to cortex [5,15–17], and these neurons are called off neurons.

Many off neurons in the inferior colliculus or more central nuclei are duration-sensitive, suggesting that they are involved in the temporal integration of auditory information and encoding of the amplitude change of the sound signal envelope [5–16]. Interestingly, these neurons are sometimes tuned to biologically important information and thereby considered to be context-dependent. For example, duration-tuned neurons in the frog auditory midbrain are commonly tuned in the range of 100 ms or less, corresponding to the duration of the frog's mating calls [6]. Many off neurons in the bat are tuned to the best frequency between 58 and 62 kHz and duration between 2 and 10 ms, which are similar to the ranges of the frequency and duration of their echolocation calls [5,7,9,16].

Previous studies, however, have not satisfactorily characterized the offset response properties particularly at the auditory cortex level. The small number of off neurons, as compared with on neurons, may hamper the detailed characterization of offset responses, particularly in terms of the place code, resulting in fragmentary information. To bridge previous fragmentary investigations, we densely map tone-burst evoked potentials over the auditory cortex and examine the overall characteristics of offset responses.

MATERIALS AND METHODS

Experimental procedure: We used a surface microelectrode array to epipially map auditory evoked potentials (AEP) in the auditory cortex of rats [18]. The array had 10 × 7 recording points in a 3.5 × 3 mm area that covered the majority of the auditory cortex including the primary, anterior, and ventral auditory field (AI, AAF and VAF). Sixty-four out of 70 recording points were selected for the recording.

Twelve adult Wister rats, weighing 200–350 g, were used. Each rat was anesthetized with ketamine (50 mg/kg, i.m.) and xylazine (10 mg/kg, i.m.), and fixed to a stereotaxic holder. The temporal bone and dura mater were partly removed to expose the auditory cortex. We inserted a reference electrode at the vertex and a ground electrode 7 mm anterior to the vertex, and mounted the surface microelectrode array on the auditory cortex.

Cortical evoked potentials from 64 recording sites were amplified simultaneously with a gain of 1000, filtered with a passband of 0.5–1500 Hz, −12 dB/octave, and digitized at a sampling rate of 200 μs. A speaker placed 20 cm from an ear,